Structural features and anti-gastric cancer activity of polysaccharides from stem, root, leaf and flower of cultivated Dendrobium huoshanense

Bing Liu, Zhen-Zi Shang, Qiang-Ming Li, Xue-Qiang Zha, De-Ling Wu, Nian-Jun Yu, Lan Han, Dai-Yin Peng, Jian-Ping Luo

PII: S0141-8130(19)37923-1

DOI: https://doi.org/10.1016/j.ijbiomac.2019.12.041

Reference: BIOMAC 14068

To appear in: *International Journal of Biological Macromolecules*

Received date: 30 September 2019

Revised date: 2 December 2019

Accepted date: 5 December 2019

Please cite this article as: B. Liu, Z.-Z. Shang, Q.-M. Li, et al., Structural features and anti-gastric cancer activity of polysaccharides from stem, root, leaf and flower of cultivated Dendrobium huoshanense, *International Journal of Biological Macromolecules*(2018), https://doi.org/10.1016/j.ijbiomac.2019.12.041

Title:

Structural features and anti-gastric cancer activity of polysaccharides from stem, root, leaf and flower of cultivated *Dendrobium huoshanense*

Authors:

Bing Liu[a,b], Zhen-Zi Shang[a,b], Qiang-Ming Li[a,b], Xue-Qiang Zha[a,b], De-Ling Wu[c], Nian-Jun Yu[c], Lan Han[a,b], Dai-Yin Peng[c], Jian-Ping Luo[a,b,*]

Affiliations:

[a] School of Food and Biological Engineering, Hefei University of Technology, Hefei 230009, China

[b] Engineering Research Center of Bio-process, Ministry of Education, Hefei University of Technology, Hefei 230009, China

[c] School of Pharmacy, Anhui University of Chinese Medicine, Hefei, 230012, China

*** Corresponding author:**

Prof. Jian-Ping Luo, School of Food and Biological Engineering, Hefei University of Technology, Hefei 230009, People's Republic of China. E-mail: jianpingluo@hfut.edu.cn.

Graphical abstract:

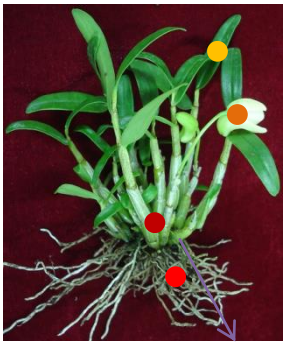

β-D-Gal*p*-1
|
6
3-*O*-acetyl
|
→[(4-β-D-Man*p*-1)x→4-β-D-Glc*p*-1→3-β-D-Man*p*-1→(4-β-D-Man*p*-1)y→4-β-D-Man*p*-1→(4-β-D-Man*p*-1)z]n→
(x + y + z = 17, n = 6)

β-D-Gal*p*-1
|
6
→[(4-β-D-Man*p*-1)x→(4-β-D-Glc*p*-1)y→3-β-D-Man*p*-1→(4-β-D-Man*p*-1)z]n→
(x + z = 9, y = 3, n = 211)

3-*O*-acetyl
|
→[(4-β-D-Man*p*-1)x→(4-β-D-Glc*p*-1)y→4-β-D-Man*p*-1→(4-β-D-Man*p*-1)z]n→
(x + z = 35, y = 12, n = 30)

β-L-Ara*f*-1 β-L-Ara*f*-1
| |
3 5
→[6-α-D-Gal*p*-1→6-α-D-Gal*p*-1→4-β-D-Man*p*-1→5-α-L-Ara*f*-1→6-α-D-Gal*p*-1→6-α-D-Gal*p*-1→3-α-L-Ara*f*-1→
6-α-D-Gal*p*-1→6-α-D-Gal*p*-1→4-β-D-Man*p*-1→4-β-D-Glc*p*-1→6-α-D-Gal*p*-1→6-α-D-Gal*p*-1]n→ (n = 6)
6
|
β-L-Ara*f*-1

Abstract:

The structure features and anti-gastric cancer activities *in vitro* of stem, root, leaf and flower polysaccharides from cultivated *Dendrobium huoshanense* were investigated systematically. Stem polysaccharide (cDHPS) was composed of →4)-β-D-Glc*p*-(1→, →4)-β-D-Man*p*-(1→, →4)-3-*O*-acetyl-β-D-Man*p*-(1→ with the molecular weight of 2.59×10^5 Da; root polysaccharide (cDHPR) was composed of →3,5)-α-L-Ara*f*-(1→, →4)-β-D-Glc*p*-(1→, →4)-β-D-Man*p*-(1→, →4,6)-β-D-Man*p*-(1→, →6)-α-D-Gal*p*-(1→ and terminal β-L-Ara*f* with the molecular weight of 1.41×10^4 Da; leaf polysaccharide (cDHPL) was composed of →4)-β-D-Glc*p*-(1→, →4)-β-D-Man*p*-(1→, →4)-3-*O*-acetyl-β-D-Man*p*-(1→, →3,6)-β-D-Man*p*-(1→ and terminal α-D-Gal*p* with the molecular weight of 2.09×10^5 Da; and flower polysaccharide (cDHPF) was composed of →4)-β-D-Glc*p*-(1→, →4)-β-D-Man*p*-(1→, →3,6)-β-D-Man*p*-(1→ and terminal α-D-Gal*p* with the molecular weight of 4.78×10^5 Da. Among these four polysaccharides, cDHPS showed the best anti-gastric cancer activity evidenced by the inhibited growth and c-myc expression as well as the enhanced apoptosis and *p*53 expression of murine forestomach carcinoma (MFC) cells, suggesting their difference in anti-gastric cancer activity should be contributed to their difference in structure features.

Keywords: *Dendrobium huoshanense* polysaccharide; Structural feature; Anti-gastric cancer activity.

1 Introduction

Dendrobium huoshanense C. Z. Tang et S. J. Cheng (traditionally called as 'Mihu') is a perennial plant of Orchidaceae family and has been used in the traditional Chinese medicine over 2000 years [1]. *D. huoshanense* contains diverse chemical constituents, mainly including polysaccharides, alkaloids, aromatic compounds and sesquiterpenoids, and possesses diverse biological functions, mainly including immunomodulatory, antioxidative, hepatoprotective, anti-cataract, neuroprotective and anti-tumor activities [2]. Since the water extract of *D. huoshanense* is traditionally consumed as a tonic with the potential of regulating gastrointestinal function, the structures and functions of the water-soluble active constituents, especially polysaccharides that account for more than 70% in water extract, have attracted much attention. In the past decade, the tissue-cultured *D. huoshanense* at different growth stages including protocorm-like bodies and micropropagated plantlets, which were grown on Murashige and Skoog medium under the controlled conditions in the sterile plant tissue rooms, were employed as materials for the isolation, purification, structural identification and bioactivity assessment of polysaccharides due to the limitation of wild resource, which results from slow growth, habitat destruction, over-collection and commercial trade [1,3-7].

In view of the fact that the tissue-cultured materials cannot be used for medicinal purpose or health care product development, great efforts have made to improve artificial cultivation technology of *D. huoshanense* since 1960 [8]. Recently, *D. huoshanense* has been successfully cultivated in its natural habitat, and the stem, leaf and flower of cultivated *D. huoshanense* as well as their water extracts have been approved as medicinal and edible materials. However, very little research has been conducted up to date on the structure and activity of polysaccharides from

cultivated *D. huoshanense*. It is not clear whether the structural feature of polysaccharides from artificially cultivated *D. huoshanense* is different from that of tissue-cultured *D. huoshanense* due to the difference in growth patterns and environments.

We previously reported the monosaccharide compositions and glycosidic linkage types of total polysaccharides from the cultivated *D. huoshanense* stems [9]. In the present study, the homogeneous polysaccharides from stem, root, leaf and flower of the cultivated *D. huoshanense* were isolated and purified, and their structure features were systematically investigated by HPGPC, FT-IR, HPLC, GC-MS and NMR techniques. Moreover, the anti-gastric cancer activity of these four polysaccharides was compared according to the regulated proliferation, apoptosis and gene expression of gastric cancer cells.

2 Materials and methods

2.1 Materials and reagents

The cultivated *D. huoshanense* plants were collected at 2016 from Huoshan (Anhui Province of China), which were grown from seedlings of seeds under artificial-sheltered forests. Murine forestomach carcinoma (MFC) cell line was purchased from Shanghai Institutes for Biological Sciences, Chinese Academy of Sciences. DEAE-Cellulose DE-52, Sephadex G-50 and Sephacryl S-400 were purchased from GE Healthcare (Uppsala, Sweden). Dimethyl sulphoxide (DMSO), methyl iodide (CH_3I) and deuterium oxide (D_2O), monosaccharide standards including D-mannose (D-Man), L-rhamnose (L-Rha), D-glucose (D-Glc), D-galactose (D-Gal) and L-arabinose (L-Ara), as well as dextran series standards including 5000, 25000, 80000, 150000, 420000 and 670000 Da were purchased from Sigma-Aldrich (St Louis, Missouri, USA). Trifluoroacetic acid (TFA), sodium borodeuteride ($NaBD_4$) and sodium periodate were obtained from Aladdin Industrial Corporation (Shanghai, China). Dulbecco's modified eagle medium/high glucose (DMEM-H) was purchased from Hyclone (Logan, Utah, USA) and fetal bovine serum (FBS) was purchased from Clark Bioscience (Richmond, Virginia, USA). CCK-8 reagent was provided by Beyotime Institute of Biotechnology (Shanghai, China). The Annexin V-FITC apoptosis assay kit was provided by BD Biosciences (San Jose, California, USA). TRI®zol was provided by Invitrogen (Carlsbad, California, USA). RevertAid First Strand cDNA Synthesis Kit was provided by Thermo Fisher Scientific (Waltham, Massachusetts, USA) and the iTaq™ Universal SYBR@ Green Master Mix kit was provided by Bio-Rad Laboratories (Hercules, California, USA). All primers were obtained from Sangon Biotech Co., Ltd (Shanghai, China). The 5-fluorouracil (5-FU) was purchased from Shanghai EKEAR Bio-tech Co., Ltd (Shanghai, China). All other reagents were from Sinopharm Chemical Reagent Co., Ltd. (Shanghai, China).

2.2 Isolation and purification of polysaccharides

The stems, roots, leaves and flowers from whole plants of cultivated *D. huoshanense* were separated firstly and then dried to constant weight in oven at 60 ℃. Fifty grams of the materials were crushed into powder and were pre-extracted with 2 L 95 % ethanol at 25 ℃ for 24 h. Subsequently, the residue was extracted three times with 2 L distilled water at 70 ℃, each for 1 h. All of the extract was filtered and centrifuged at 5000 g for 20 min at 4 ℃. The supernatant was concentrated by vacuum rotary evaporator under reduced pressure at 60 ℃ and precipitated with ethanol at a final concentration of 80 % (v/v) allowing to stand overnight at 25 ℃. The α-amylase (46 U/mL) of 50 μL was added into the precipitate which was dissolved in 1 L distilled water to hydrolyze starch at 60 ℃ for 1 h. The hydrolyzed mixture was collected by centrifuging at 5000 g for 20 min at 4 ℃. The supernatant, after concentrated by vacuum rotary evaporator under reduced pressure at 60 ℃, was mixed with ethanol at a final concentration of 80 % (v/v) to obtain the precipitate at 25 ℃ for 24 h. The resulting precipitate was dissolved in distilled water and lyophilized at −50 ℃ below 20 Pa for 48 h to yield the crude polysaccharides. Dissolved crude polysaccharide (10 % w/v) in distilled water was fractionated on DEAE-Cellulose DE-52 anion-exchange column (1.6 cm × 60 cm) through stepwise elution with pure water and NaCl solutions of 0.1-0.5 M at a flow rate of 5 mL/min. Fractions from water elution were further purified through gel permeation chromatography on a Sephadex G-50 column (1.6 cm × 80 cm) or Sephacryl S-400 column (1.6 cm × 80 cm) with pure water elution. After concentrated by vacuum rotary evaporator under reduced pressure at 60 ℃, dialyzed at 25 ℃ for 24 h (molecular weight cut off of 3500 Da) and lyophilized at −50 ℃ below 20 Pa for 48 h, the polysaccharides including cDHPS from stems, cDHPR from roots, cDHPL from leaves and cDHPF from flowers

of cultivated *D. huoshanense* were obtained.

2.3 Measurement of physicochemical properties

The carbohydrate content was determined by phenol-sulfuric acid method [10]. The *O*-acetyl group content was determined by hydroxylamine colorimetry [11]. The aqueous solutions (2 mg/mL) of polysaccharides were scanned on a TU-1901 UV-Vis spectrophotometer (Persee, Beijing, China) within the wavelength range of 190 ~ 400 nm.

2.4 HPGPC and FT-IR analysis

High performance gel permeation chromatography (HPGPC) was used to determine the homogeneity and the relative molecular weight (Mw) of polysaccharide. Agilent 1260 Infinity system equipped with the TSK G5000PWXL (7.8 mm × 300 mm) column under the circumstance of 35 °C was used to determine the retention times of samples with refractive index detector (RID). The ultrapure water was used as mobile phase with a flow rate of 0.5 mL/min. The retention time of dextran series standards of 5000, 25000, 80000, 150000, 420000 and 670000 Da was measured under the same conditions. Then the molecular weight standard curve was fitted using Agilent GPC data analysis in ChemStation B.04.03 and the Mw of cDHPS, cDHPR, cDHPL and cDHPF was calculated according to the standard curve.

For FT-IR analysis, the dried polysaccharide samples were mixed with KBr powder and pressed into flake, and then scanned on Nicolet 6700 spectrometer (Thermo Nicolet, Madison, WI, USA) to record FT-IR spectrum ranging from 4000 to 400 cm^{-1}.

2.5 Monosaccharide composition analysis

Five milligrams of dried samples were dissolved in 3 mL of 2 M trifluoroacetic acid (TFA) and 1 mL of glucosamine hydrochloride (0.96 mg/mL) was added as an internal standard. The

mixed solution was hydrolyzed at 110 ºC for 4 h. After the solution was cooled to room temperature, the reaction mixture was evaporated at 60 ºC under reduced pressure to remove TFA and the residue was dissolved in 4 mL of ultrapure water. Then, 400 μL of the sample solution was added with 400 μL of 1-phenyl-3-methyl-5-pyrazalone (PMP) methanol solution (0.5 M) and 400 μL of NaOH solution (0.3 M), and was permitted to react in water bath at 70 °C for 100 min. Subsequently, the sample solution was washed three times with chloroform following the addition of HCl solution (0.3 M) with 500 μL, and the resulting aqueous layer was collected by centrifugation at 500 g at 4 °C for 15 min and filtration with 0.22 μm membrane to obtain the PMP-labeled samples for HPLC analysis on Agilent 1260 Infinity system equipped with a UV detector. The mobile phase was acetonitrile-0.02 M ammonium acetate solution (2 : 8, v/v) with a flow rate of 1 mL/min and the Agilent XDB-C18 column (250 mm × 4.6 mm) was used at the circumstance of 25 ºC [12].

2.6 Periodate oxidation and Smith degradation

The dried samples (20 mg) were dissolved in 10 mL double distilled water and reacted with 30 mM $NaIO_4$ (10 mL) under 4 °C in the dark. Ten microliters of the reaction solution were monitored every 6 h with the absorption at 223 nm until a constant value and the un-reacted $NaIO_4$ was quenched with ethylene glycol. Then the production of formic acid was determined by titration with 0.1 M NaOH (phenolphthalein as an indicator). Further, the freshly prepared $NaBH_4$ solution (1 M) was added into reaction solution to reduce polyaldehyde and the resulting polyol was desalted by dialysis bag of molecular weight cutoff of 3500 Da followed by lyophilization at −50 °C below 20 Pa for 48 h. The lyophilizate was dissolved in 4 M trifluoroacetic acid (TFA), hydrolyzed at 110 °C for 4 h and acetylated with pyridine and acetic anhydride. The acetylated

products were extracted by dissolving them with an appropriate amount of dichloromethane and the dichloromethane layer was analyzed by GC-MS following by dehydration with anhydrous sodium sulfate and filtration with 0.22 μm organic membrane [13]. Agilent GC7890A-MSD5975C instrument equipped with a HP-5 capillary column (30 m × 0.32 mm ×0.25 μm) was used. The inlet temperature was 280 ℃ and the procedure of column temperature was set as follows: first 150 ℃ for 1 min, then rise to 200 ℃ at 10 ℃/min, finally increase to 270 ℃ at 4 ℃/min. The flow rate of helium was 1 mL/min and temperature of ion source was 150 ℃.

2.7 Methylation analysis

The methylation method was carried out according to the modified Ciucanu method [14]. The dried sample (20 mg) was dissolved in 5 mL DMSO, followed by the addition of 200 mg NaOH powder which was fully ground in liquid nitrogen and the sonication at the frequency of 90 KHz for 50 min at 35 ℃. Then, the mixture in ice bath was treated with methyl iodide in the dark. The complete methylation was detected by FT-IR according to the disappearance of hydroxyl groups. All the above procedures were performed under a nitrogen flow condition. Then the dried methylated products were depolymerized with formic acid at 100 ℃ for 3 h followed by a further acid hydrolysis with 4 M TFA at 110 ℃ for 4 h. Lastly, the partially methylated sugar residues were reduced with $NaBD_4$, acetylated with pyridine and acetic anhydride, and analyzed by GC-MS as described in Section 2.6.

2.8 NMR analysis

One hundred milligrams of the samples were exchanged with deuterium oxide (D_2O) by lyophilizing for three times. The lyophilizate was dissolved in 99.9 % D_2O containing sodium

4,4-dimethyl-4-silapentan-sulfonate (DSS) and transferred to the NMR tube (5 mm, Wilmad-Lab Glass, Buena, NJ, USA) after filtration of 0.22 μm membrane. All NMR spectra including ^{1}H (298 K and 328 K), ^{13}C, ^{1}H-^{1}H COSY, HSQC, HMBC, TOCSY, ROESY were recorded on a Varian VNMRS 600 MHz superconducting nuclear magnetic resonance spectrometer with a 5 mm OneNMR probe (Agilent Technologies Inc., USA). The operating frequencies of ^{1}H NMR and ^{13}C NMR were 599.81 MHz and 150.84 MHz. The 1D NMR spectra were recorded using s2pul pulse sequence and the 2D NMR spectra were acquired using gCOSY, zTOCSY, HSQCAD, gHMBCAD and ROESYAD pulse sequences, respectively.

2.9 Assessment of cell viability

The MFC cells were seeded in 96 well plates at a density of 5×10^{3} cells/well. After 24 h adhesion, the cells were incubated with cDHPS, cDHPR, cDHPL or cDHPF at the concentrations of 0.025, 0.05, 0.1, 0.2, 0.4, 0.8, 1.0, 1.5, 2.0 and 2.5 mg/mL, respectively. Medium and 5-Fu (0.1 mg/mL) were served as the normal control (NC) and positive control (PC), respectively. After incubation for 24 h at 37 °C in a humidified incubator with 5 % CO_2, CCK-8 reagent (10 μL/well) was added into each well and the plates were further incubated for 2 h. Subsequently, the optical density (OD) values were measured at 450 nm on the Multiskan FC microplate reader (Thermo Fisher Scientific, Finland). The cell viability was calculated as follows: the cell viability (%) = $(1–OD_{experiment}/OD_{blank\ control}) \times 100$ %. All assays were separately repeated three times and the half maximal inhibitory concentration (IC_{50}) was also calculated.

2.10 Detection of cell apoptosis

The MFC cells were seeded at a concentration of 1×10^{6} cells/well into a 6-cell plate and incubated for 12 h at 37 °C in a humidified incubator with 5 % CO_2 before the addition of cDHPS,

cDHPR, cDHPL or cDHPF at the concentration of 0.025, 0.05, 0.1, 0.2, 0.4, 0.8, 1.0 and 1.5 mg/mL for 24 h, respectively. Medium and 5-Fu (0.1 mg/mL) were served as the normal control (NC) and positive control (PC), respectively. The cells were harvested by centrifuging at 2000 g for 10 min at 4 °C after digested with EDTA-free trypsin. Then the cells were washed with pre-cooled phosphate buffer (0.01 M, pH 7.4) and resuspended in 300 μL 1 × binding buffer provided by the apoptosis assay kit. Annexin V-FITC (5 μL) and 5 μL of propidiom iodide (PI) from assay kit were added to the cell solution and incubated for 30 min in the dark at room temperature. The sample was detected by MoFlo$^{@}$XDP flow cytometry (Beckman coulter, USA) and the percentages of early and late apoptotic rates were quantified by FlowJo software 7.6.

2.11 Quantitative RT-PCR analyses

The MFC cells were seeded into a 24-well plate at a density of 1×10^{6} cells/mL. As described above, MFC cells were treated with cDHPS, cDHPR, cDHPL or cDHPF at the concentration of 0.025, 0.05, 0.1, 0.2, 0.4, 0.8, 1.0 and 1.5 mg/mL for 24 h incubation at 37 °C in a humidified incubator with 5 % CO_2, respectively. Medium and 5-Fu (0.1 mg/mL) were served as the normal control (NC) and positive control (PC), respectively. The TRI®zol reagent was employed to extract total RNA, which was reverse-transcribed using RevertAid First Strand cDNA Synthesis Kit. The mixture was incubated in PCR system (Applied Biosystems GeneAmp 2400, Thermo Fisher, USA) at 42 °C for 60 min, followed by incubating at 70 °C for 5 min. PCR reaction was performed on a iQ5 Real Time PCR system (BIO-RAD, USA) with a reaction volume of 20 μL containing 10 μL 2 × iTaq^{TM} Universal SYBR$^{@}$ Green Master Mix, 0.6 μL forward primer, 0.6 μL reverse primer, 1 μL cDNA and 7.8 μL RNase-Free ddH_2O. Primers were designed as follows: 5’-TGTGGAGTATTTGGATGACA-3’ (Forward) and 5’-GAACATGAGTTTTTTATGGC-3’

(Reverse) for the *p*53 gene; 5'-GAACAAGAAGATGAGGAAGA-3' (Forward) and 5'-AGTTTGTGTTTCAACTGTTC-3' (Reverse) for the c-myc gene; 5'-GAGACCTTCAACACCCAGCC-3' (Forward) and 5'- GCGGGGCATCGGAACCGCTCA-3' (Reverse) for the β-actin gene (use as an internal control). The thermal cycling procedures were set as follows: initial denaturation at 94 ℃ for 1 min followed by 40 cycles of denaturation at 95 ℃ for 20 s, annealing at 60 ℃ for 1 min, extension at 72 ℃ for 2 min, and a final extension was at 72 ℃ for 6 min.

2.12 Statistical analysis

All experiment results were expressed as the mean ± SE. All data were analyzed by one-way analysis of variance (ANOVA) and multiple comparisons were performed by SPSS 23.0 software.

3 Results

3.1 Physicochemical properties of stem, root, leaf and flower polysaccharides

After water extraction, ethanol precipitation and α-amylase digestion as well as purification on anion-exchange and gel permeation chromatography, polysaccharides including cDHPS from stems, cDHPR from roots, cDHPL from leaves and cDHPF from flowers were obtained with the yield of 13.14±1.44 %, 0.81±0.46 %, 3.68±0.83 % and 2.77±0.37 %, respectively. The carbohydrate content of these polysaccharides was over 95 %, with *O*-acetyl group contents ranging from 0.39 % to 2.78% (Table 1). The UV scanning (Supplemental Figure 1) suggested that these polysaccharides were free of proteins and nucleic acids. In the HPGPC spectra (Fig. 1A, 2A, 3A and 4A), cDHPS, cDHPR, cDHPL and cDHPF all exhibited a symmetrical peak, indicating their homogeneity. According to standard curve ($y = - 0.3122 x + 10.39$, $R^2 = 0.9976$), the relative molecular weights of cDHPS, cDHPR, cDHPL and cDHPF were 2.59×10^5 Da, 1.41×10^4 Da, 2.09×10^5 Da and 4.78×10^5 Da, respectively.

FT-IR spectra (Fig. 1B, 2B, 3B and 4B) demonstrated that cDHPS, cDHPR, cDHPL and cDHPF had the characteristic peaks of polysaccharides. The broad intense peak at around 3700 cm^{-1}—3100 cm^{-1} was attributed to the stretching vibration of -OH. The peaks at around 2930 cm^{-1} and 2880 cm^{-1} were from the stretching vibration of C-H. Characteristic absorptions for the C-O vibration of C-O-C and C-O-H in the pyranose rings of polysaccharides were occurred between 1250 cm^{-1} and 950 cm^{-1}. The peaks between 1400 cm^{-1} and 1200 cm^{-1} were from the symmetric C-H bending vibration, the peak at 1740 cm^{-1} from the stretching vibration of C=O and the peak at 1245 cm^{-1} from the stretching vibration of C-O. In addition, the peak at 895 cm^{-1} for β-glycosidic bond in all polysaccharides could be found in FT-IR spectra.

3.2 Structural characterization of stem, root, leaf and flower polysaccharides

3.2.1 cDHPS

cDHPS was mainly composed of D-Man and D-Glc in a molar ratio of 3.04 : 1.00 (Supplemental Figure 2). The analysis of periodate oxidation found that 1.77 mol $NaIO_4$ was consumed without the production of formic acid, indicating the existence of (1→2), (1→2, 6) or (1→4), (1→4,6)-linked glycosidic bonds. The oxidized products after reduced, hydrolyzed and acetylated, were subjected to GC-MS analysis (Supplemental Figure 3), and the presence of ethylene glycol and erythritol confirmed the existence of (1→4) or (1→4,6)-linked glycosidic bonds in cDHPS. Methylation analysis found two peaks in the TIC profile of cDHPS (Supplemental Figure 4 and Supplemental Table 1), which were identified as 2,3,6-Me_3-Man*p* and 2,3,6-Me_3-Glc*p* with a molar ratio of 2.88 : 1.00. These results suggested that cDHPS contained two glycosidic linkages, i.e. 1,4-linked Man*p* and 1,4-linked Glc*p*.

In order to avoid the interference of deuterium oxide (D_2O) solvent peak, the analysis of ^1H NMR spectrum was carried out at temperature of 298 K (Fig. 1C) and 328 K (Fig. 1D), respectively, and three anomeric protons were found at δ 4.52 ppm, δ 4.75 ppm and δ 4.77 ppm, which were named as residue A_S, B_S and C_S.

The residue A_S should be β-configuration on the basis of its anomeric proton signal at δ 4.52 ppm with a large coupling constant value of $^3J_{1,2}$(~7.42 Hz), which was supported by its anomeric carbon signal at δ 105.49 in ^{13}C NMR spectrum (Fig. 1E) and the existence of a cross signal at δ 4.52/105.49 ppm in HSQC spectrum (Fig. 1F). According to the chemical shift of H-1, the cross signal at δ 4.52/3.33 ppm (H-1/H-2) and δ 3.33/3.62 ppm (H-2/H-3) could be discerned in the COSY spectrum (Fig. 1G). Although H-3 (δ 3.63 ppm) and H-4 (δ 3.62 ppm) were very close to

each other and almost close to the diagonal, H-4/H-5 (δ 3.63/3.56 ppm) could be easily found based on the characteristics of H-5. In the TOCSY spectrum (Supplemental Figure 5A), the ^{1}H chemical shifts were further confirmed by the spatial relationship among protons inside the residue with the cross-signals of H-1/H-2 (δ 4.52/3.33 ppm), H-1/H-3 (δ 4.52/3.62 ppm), H-1/H-4 (δ 4.52/3.63 ppm), H-1/H-6a (δ 4.52/3.91 ppm) and H-1/H-6b (δ 4.52/3.82 ppm). In the HSQC spectrum (Fig. 1F), cross-peaks for H-2/C-2 (δ 3.33/75.49 ppm), H-3/C-3 (δ 3.62/76.77 ppm), H-4/C-4 (δ 3.63/80.24 ppm) and H-5/C-5(δ 3.56/77.72 ppm) could be found while the peak for H-6/C-6 was overlapped with other residue signals. All chemical shifts of the corresponding carbons were confirmed in the ^{13}C NMR spectrum. Thus, the residue A_S was established as →4)-β-D-Glc*p*-(1→ as comparing above analysis with literature's data [15], and the detail information was listed in Table 2.

As for the residue B_S, its anomeric proton at δ 4.75 ppm in the ^{1}H NMR spectrum (Fig. 1D) and anomeric carbon at δ 102.87 ppm in the ^{13}C NMR spectrum (Fig. 1E), which was evidenced by the dominant coupling signal at δ 4.75/102.87 ppm in the HSQC spectrum (Fig. 1F), suggested it was β-configuration. In the COSY spectrum (Fig. 1G), proton chemical shifts of H-1/H-2 (δ 4.75/4.11 ppm), H-2/H-3 (δ 4.11/3.72 ppm) and H-4/H-5 (δ 3.75/3.50 ppm) were further assigned although the chemical shifts of H-3 and H-4 were very close to each other as found for residue A_S. Based on the proton chemical shifts, the correlations between H-1/C-1 (δ 4.75/75.49 ppm), H-2/C-2 (δ 4.11/72.61 ppm), H-3/C-3 (δ 3.72/74.82 ppm), H-4/C-4 (δ 3.78/79.18 ppm) and H-5/C-5 (δ 3.50/77.77 ppm) could be found in the HSQC spectrum (Fig. 1F), where the cross-peak of H-6/C-6 was overlapped with other peaks. Comparing above analysis with literature's data [15], it could be assumed that the residue B_S should be →4)-β-D-Man*p*-(1→, and

all signals of H and C resonances were shown in Table 2.

As the residue B_S, the residue C_S also existed as the β-linkage, which was supported by the anomeric proton at δ 4.77 ppm in ^{1}H NMR (Fig. 1D), the anomeric carbon at δ 101.99 ppm in ^{13}C NMR (Fig. 1E) and their coupling signal at δ 4.77/101.99 ppm in HSQC (Fig. 1F). Further, the signals for other H and C, which were shown in Table 2, were assigned according to COSY spectrum (Fig. 1G) and HSQC spectrum (Fig. 1F). Compared with the residue B_S, the signal for H-3 of the residue C_S shifted to the lower field, while its C-2 and C-4 signals moved toward the higher field. These changes may be attributed to the presence of *O*-acetyl group, which was revealed both by ^{1}H NMR spectrum, where three hydrogens on the methyl group in *O*-acetyl group occurred around δ 2.19 ppm, δ 2.18 ppm and δ 2.15 ppm (Fig. 1C), and by ^{13}C NMR spectrum, where the resonances of carbonyl carbons and methyl carbons in *O*-acetyl group occurred at δ 174.17 ppm and δ 23.04 ppm (Fig. 1E). Considering the methylation analysis of glycosidic linkages, the residue C_S could be assigned as →4)-3-*O*-acetyl-β-D-Man*p*-(1→.

In the upper left region of the HMBC spectrum (Fig. 1H), it was easy to find the inter-residual cross peaks between A_S H-1/ A_S C-4 (δ 4.75/80.24 ppm), A_S H-1/ C_S C-4 (δ 4.52/ 75.70 ppm), and C_S H-1/ A_S C-4 (δ 4.77/79.18 ppm). Thus, the possible repeat unit of cDHPS could be inferred as follows:

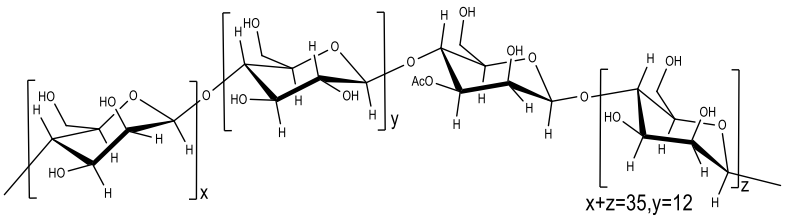

3.2.2 cDHPR

cDHPR consisted of D-Man, D-Glc, D-Gal and L-Ara in a molar ratio of 2.38 : 1.00 : 8.49 :

5.23 (Supplemental Figure 2). Further, the results of periodate oxidation and Smith degradation experiment (Supplemental Figure 3) and methylation analysis (Supplemental Figure 4 and Supplemental Table 1) implied that the glycosidic linkages of cDHPR included 1-linked-Ara*f*, 1,4-linked Man*p*, 1,4-linked Glc*p*, 1,6-linked Gal*p*, 1,4,6-linked Man*p* and 1,3,5-linked Ara*f* in a molar ratio of 3.55 : 1.74 : 1.52 : 8.37 : 1.00 : 2.41.

In the ^{1}H NMR spectra at 298 K (Fig. 2C) and at 328 K (Fig. 2D), the signals for anomeric protons of cDHPR were found at δ 5.24 ppm, δ 4.49 ppm, δ 4.73 ppm, δ 5.02 ppm, δ 4.57 ppm and δ 5.08 ppm, which were named as residue A_R, B_R, C_R, D_R, E_R and F_R, respectively. Among these residues, B_R and C_R were basically the same as the residue A_S and B_S of cDHPS, and were respectively assigned as →4)-β-D-Glc*p*-(1→ and →4)-β-D-Man*p*-(1→ according to the information from 1D and 2D NMR (Fig. 2 and Table 2).

For the residue A_R, the anomeric proton at δ 5.24 ppm (Fig. 2C and 2D), the anomeric carbon at δ 111.82 ppm (Fig. 2E) and their coupling signal at δ 5.24/111.82 ppm (Fig. 2F) indicated that it presented as α-configuration. In COSY (Fig. 2G), the cross signals for H-1/H-2, H-2/H-3, H-3/H-4 and H-4/H-5 were found at δ 5.24/3.97 ppm, δ 3.97/3.96 ppm, δ 3.96/4.15 ppm and δ 4.15/3.80 ppm with the assistance of TOCSY spectrum (Supplemental Figure 5C). Accordingly, the cross signals for H-2/C-2, H-3/C-3, H-4/C-4 and H-5/C-5 were found at δ 84.53/3.97 ppm, δ 85.94 /3.96 ppm, δ 82.98 /4.15 ppm and δ 68.51 /3.80 ppm in HSQC. Thus, the residue A_R could be attributed to →3,5)-α-L-Ara*f*-(1→ based on the methylation analysis and literature data [16].

For the residue D_R, the anomeric region signal at δ 5.02 ppm (Fig. 2C and 2DB), δ 101.69 ppm (Fig. 2E) and their coupling signal at δ 5.02/101.69 (Fig. 2F) were found in ^{1}H NMR, ^{13}C

NMR and HSQC, respectively. Furthermore, signals for H-2 to H-5 and C-2 to C-5 were found in sequence in COSY (Fig. 2G) and HSQC (Fig. 2F), respectively. Consulting methylation analysis and literature data [17], the residue D_R could be designated as β-L-Ara*f*-(1→.

The residue E_R existed as β-configuration, which was inferred based on chemical shifts of anomeric proton at δ 4.57 ppm (Fig. 2C and 2D), anomeric carbon at δ 100.21 ppm (Fig. 2E) and their coupling-signal at δ 4.57 ppm/100.21 ppm (Fig. 2F). In COSY (Fig. 2G), the H-1/H-2 (δ 4.57 ppm/3.96 ppm), H-2/H-3 (δ 3.96 ppm/4.08 ppm), H-3/H-4 (δ 4.08 ppm/3.77 ppm), H-4/H-5 (δ 3.77 ppm/3.78 ppm) and H-5/H-6 (δ 3.78 ppm/3.95 ppm) were found. This assignment was supported by the correlations between δ 3.96 ppm/70.98 ppm (H-2/C-2), δ 4.08 ppm/70.35 ppm (H-3/C-3), δ 3.77 ppm/78.22 ppm (H-4/C-4), δ 3.78 ppm/69.91 ppm (H-5/C-5) and δ 3.78 pm/68.36 ppm (H-6/C-6) in HSQC (Fig. 2F). Compared with the residue C_R, the chemical shift of C-6 (δ 68.36 ppm) in the residue E_R moved to the lower field, suggesting the occurrence of glycosylation [18]. Thus, the residue E_R should be →4,6)-β-D-Man*p*-(1→.

Residue F_R had anomeric proton at δ 5.08 ppm (Fig. 2C and 2D) and anomeric carbon at δ 98.73 ppm (Fig. 2E), as well as their cross-signal at δ 5.08/98.73 ppm in HSQC (Fig. 2F), indicating it was α-configuration residue. Starting from H-1, the signals of H-2 (δ 3.99 ppm), H-3 (δ 3.69 ppm), H-4 (δ 4.06 ppm), H-5 (δ 3.92 ppm), H-6a (δ 3.66 ppm) and H-6b (δ 3.76 ppm) were found in COSY (Fig. 2G) and TOCSY (Supplemental Figure 5C). Correspondingly, the chemical shifts from C-2 to C-6 (δ 70.68 ppm, δ 69.13 ppm, δ 68.99 ppm, δ 71.90 ppm and δ 66.22 ppm) were found in HSQC. Referring to the literature data[19], the residue F_R could be assigned as →6)-α-D-Gal*p*-(1→, where the downfield shift of C-6 (δ 66.22 ppm) signal suggested the formation of glycosidic bond.

The linkage sequence of glycosyl residues in cDHPR was further derived according to the cross-peaks in HMBC (Fig. 2H). These cross-peaks included δ 5.24/68.99 ppm, δ 4.49/66.22 ppm, δ 4.73/68.51 ppm, δ 4.57/80.98 ppm, δ 5.02/68.36 ppm, δ 5.02/68.51 ppm, δ 5.02/85.94 ppm, δ 5.08/66.22 ppm, δ 5.08/78.22 ppm and δ 5.08/79.58 ppm, indicating the linkages of A_R H-1 / F_R C-4, B_R H-1/ F_R C-6, C_R H-1/ A_R C-5, E_R H-1 / B_R C-4, D_R H-1/E_R C-6, D_R H-1/A_R C-5, D_R H-1/A_R C-3, F_R H-1/F_R C-6, F_R H-1/E_R C-4 and F_R H-1/C_R C-4 in cDHPR, which were evidenced by the ROESY experiment (Supplemental Figure 5D). Accordingly, the structure of cDHPR could be proposed to be composed of →3,5)-α-L-Ara*f*-(1→, →4)-β-D-Glc*p*-(1→, →4)-β-D-Man*p*-(1→, →4,6)-β-D-Man*p*-(1→ and →6)-α-D-Gal*p*-(1→ as the backbone, along with the branches consisting of β-L-Ara*f*-(1→. The possible repeat unit of cDHPR was shown as follows:

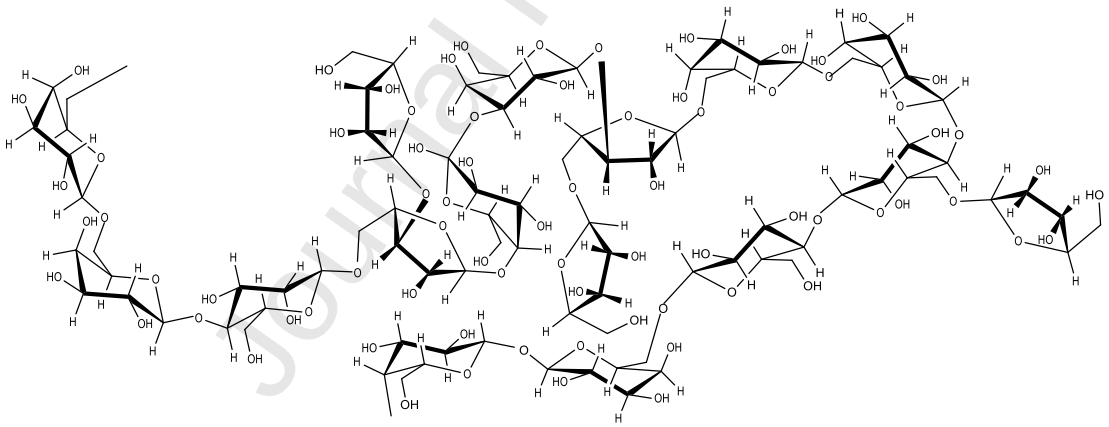

3.2.3 cDHPL

cDHPL comprised a large proportion of D-Man and a trace of D-Glc and D-Gal in a molar ratio of 19.15 : 1.32 : 1.00 (Supplemental Figure 2). Methylation analysis (Supplemental Figure 4 and Supplemental Table 1) suggested the glycosidic linkage types of cDHPL included 1-linked-Gal*p*, 1,4-linked Man*p*, 1,4-linked Glc*p* and 1,3,6-linked Man in a molar ratio of 1.00 :

17.89 : 1.33 : 1.58, which was supported by the periodate oxidation and Smith degradation experiment (Supplemental Figure 3).

The ^{1}H NMR experiment at 298 K (Fig. 3C) and at 328 K (Fig. 3D) showed the anomeric protons of cDHPL were at δ 4.48 ppm, δ 4.73 ppm, δ 4.82 ppm, δ 5.17 ppm and δ 4.76 ppm, which were marked as residue A_L, B_L, C_L, D_L and E_L. Correspondingly, the anomeric carbons of these residues were found at δ 105.04 ppm, δ 102.69 ppm, δ 101.13 ppm, δ 96.51 ppm and δ 96.35 ppm were obtained in the ^{13}C NMR experiment (Fig. 3E). Among these residues, the identification of residue A_L, B_L and C_L was similar to that of cDHPS, and they were →4)-β-D-Glc*p*-(1→, →4)-β-D-Man*p*-(1→ and →4)-3-*O*-acetyl-β-D-Man*p*-(1→, respectively, and all signals of H and C resonances were shown in Table 2.

For the residue D_L, anomeric proton at δ 5.17 ppm (Fig. 3C and 3D), anomeric carbon at δ 96.51 ppm (Fig. 3E) and their coupling signal at δ 5.17/96.51 ppm (Fig. 3F) indicated it was α-configuration residue. According to H-1 (δ 5.17 ppm), the chemical shifts from H-2 to H-6 can be found in COSY (Fig. 3G) and TOCSY (Supplemental Figure 5E). Subsequently, the ^{13}C chemical shifts were determined from the cross-peaks of H and C in HSQC. Thus, the residue D_L was identified as α-D-Gal*p*-(1→ based on its unique signal of C-2 (δ 67.95 ppm) and C-6 (δ 61.10 ppm) [20].

The residue E_L existed as β-configuration according to the anomeric proton at δ 4.76 ppm (Fig. 3D), the anomeric carbon at δ 96.35 ppm (Fig. 3E) and their coupling signal at δ 4.76/96.35 ppm in HSQC (Fig. 3F). The correlation signals of different protons as well as cross signals between protons and carbons could be found in COSY (Fig. 3G) and HSQC (Fig. 3F). The downfield shifts of C-3 (δ 77.53 ppm) and C-6 (δ 69.56 ppm) with reference to the pertinent data

[21] indicated the occurrence of replacement, suggesting that the residue E_L was →3,6)-β-D-Man*p*-(1→.

The linkage sequence of different residues in cDHPL was inferred from the correlations between C and H in HMBC (Fig. 3H). The cross-peaks between A_L H-1 and E_L C-3 at δ 4.48/77.53 ppm, B_L H-1 and A_L C-4 at δ 4.73/79.83 ppm , B_L H-1 and C_L C-4 at δ 4.73/75.83 ppm , B_L H-1 and B_L C-4 at δ 4.73/79.26 ppm, C_L H-1 and B_L C-4 at δ 4.82/79.26 ppm, E_L H-1 and B_L C-4 at δ 4.76/79.26 ppm indicated that the backbone of cDHPL could be composed of →4)-β-D-Glc*p*-(1→, →4)-β-D-Man*p*-(1→, →4)-3-*O*-acetyl-β-D-Man*p*-(1→ and →3,6)-β-D-Man*p*-(1→. The cross-peak between D_L H-1 and E_L C-6 at δ 5.17/69.56 ppm indicated that the residue D_L as the branch was attached to the C-6 of residue E_L. These results were confirmed by the ROESY experiment (Supplemental Figure 5F), and the possible repeat unit of cDHPL was presented as follows:

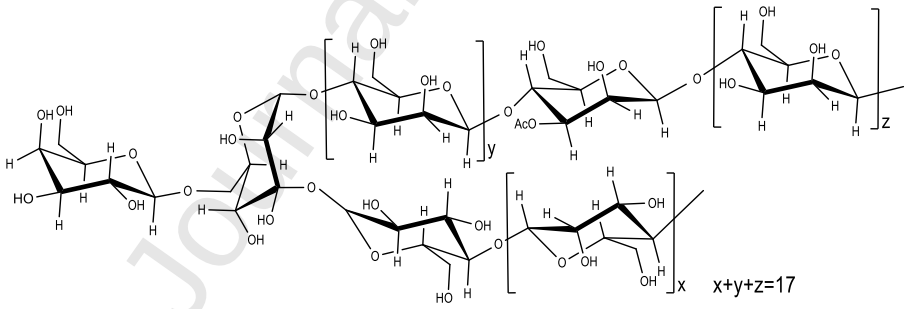

3.2.4 cDHPF

cDHPF was composed of D-Man, D-Glc and D-Gal with molar ratio of 9.68 : 3.26 : 1.00 (Supplemental Figure 2). Mthylation analysis (Supplemental Figure 4 and Supplemental Table 1), with the assistance of periodate oxidation and Smith degradation experiment (Supplemental Figure 3), indicated that the glycosidic linkage types of cDHPF included 1-linked-Ara*f*, 1,4-linked Man*p*, 1,4-linked Glc*p*, and 1,3,6-linked Man*p* in a molar ratio of 1.00 : 9.18 : 2.65 :

1.12.

According to ^{1}H NMR (Fig. 4C and 4D) and ^{13}C NMR (Fig. 4E) experiments, four residues, i.e. A_F, B_F, C_F and D_F, were found, and their assignment process were consistent with the residue A_S of cDHPS, the residue B_S of cDHPS, the residue D_L of cDHPL and theresidue E_L of cDHPL, respectively. Based on the signals of all H and C (Table 2), which inferred from 2D NMR (Fig. 4F-H and Supplemental Figure 5G-H), A_F, B_F, C_F and D_F were →4)-β-D-Glc*p*-(1→, →4)-β-D-Man*p*-(1→, α-D-Gal*p*-(1→ and →3,6)-β-D-Man*p*-(1→, respectively. The inter-residual cross-peaks, i.e. A_F H-1/D_F C-3 (δ 4.49/77.25 ppm), B_F H-1/A_F C-4 (δ 4.74/80.72 ppm), B_F H-1/B_F C-4 (δ 4.74/80.22 ppm), C_F H-1/D_F C-6 (δ 5.17/69.06 ppm) and D_F H-1/B_F C-4 (δ 4.90/80.22 ppm), were easy to be found in HMBC (Fig. 4H) and confirmed by the ROESY experiment (Supplemental Figure 5H). Accordingly, the structure of cDHPF could be composed of →4)-β-D-Glc*p*-(1→, →4)-β-D-Man*p*-(1→ and →3,6)-β-D-Man*p*-(1→ as the backbone with the branch consisting of α-D-Gal*p*-(1→, and the possible repeat unit was proposed as follows:

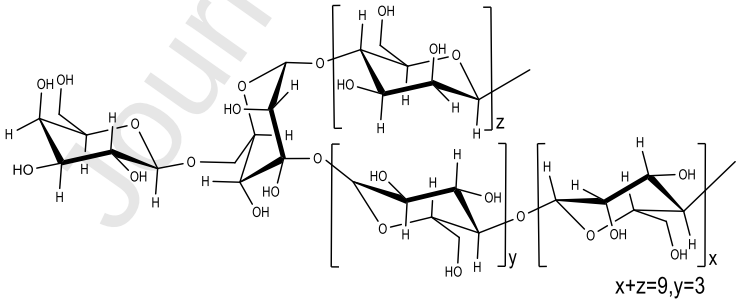

3.3 Effects of different polysaccharides on MFC cell viability

The treatment with cDHPS, cDHPR, cDHPL and cDHPF in a certain range of concentrations could inhibited the proliferation of gastric cancer MFC cells, and their concentrations showing the highest inhibition effect were 0.2 mg/mL for cDHPS, 0.8 mg/mL for cDHPL, 1.0 mg/mL for cDHPF and 2.0 mg/mL for cDHPR, respectively (Fig. 5). Obviously, among these four

polysaccharides, cDHPS had the best inhibitory effect on the proliferation of MFC cells with an IC_{50} of 0.327 mg/mL followed by cDHPL with an IC_{50} of 1.524 mg/ mL. cDHPF and cDHPR only displayed weak inhibitory effects, and their IC_{50} values (3.588 mg/mL and 4.651 mg/mL, respectively) were significantly higher than those of cDHPS and cDHPL.

3.4 Effects of different polysaccharides on the MFC cell apoptosis

MFC cell apoptosis was analyzed with Annexin V-FITC & PI assay by flow cytometry, and the total percentage of apoptosis both at early stage and late stage was presented in upper right area and lower right area of Fig. 6A-F, respectively. These data showed that cDHPS could significantly induce cell apoptosis in the tested concentration range, and the total apoptosis rate rose from 16 % at 25 μg/mL to 25.05 % at 100 μg/mL, which was significantly higher than that of untreated MFC cells (2.12 ± 0.48 %) and was very near to that of positive group (28.45 ± 0.98%). Compared to cDHPS, cDHPL and cDHPF induced a lower apoptosis of MFC cells although the percentage of total apoptotic cells was higher than that of untreated MFC cells. The highest apoptosis for cDHPL occurred at 800 μg/mL and for cDHPF at 1.0 mg/mL. cDHPR only showed a tiny effect on the apoptosis of MFC cells, and no significant difference was found between cDHPR treatment at all tested concentrations and the normal control group. These results suggested that the cDHPS had the best ability to induce gastric cancer cell apoptosis as compared to cDHPR, cDHPL and cDHPF ($p < 0.01$) (Fig. 6G).

3.5 Effects of different polysaccharides on the gene expression of *p*53 and c-myc in MFC cells

qRT-PCR analysis showed that cDHPS at all tested concentrations could significantly promote the gene expression of wild-type tumor suppressor gene *p*53 (Fig. 7A) and inhibit the

expression of proto-oncogene c-myc (Fig. 7B) in MFC cells, which was similar to that of the positive control even if the concentration of cDHPS was lowered to 0.025 mg/mL. Compared to cDHPS, cDHPL enhanced the expression of *p*53 ($p<0.05$) and decreased the expression of c-myc ($p<0.05$) at the concentration of more than 0.4 mg/mL, and cDHPF displayed markedly influence on the gene expression of *p*53 and c-myc at the concentration of more than 0.8 mg/mL. However, cDHPR had no significant effect on *p*53 and c-myc gene expression at all tested concentration as compared to the normal control. Obviously, cDHPS showed the strongest effect on up-regulated expression of *p*53 gene and down-regulated expression of c-myc gene.

4 Discussion

In the current study, four homogeneous polysaccharides, named as cDHPS, cDHPR, cDHPL and cDHPF, were isolated and purified from stem, root, leaf and flower of artificially cultivated *D. huoshanense*, respectively. Based on the analysis of HPLC, FT-IR, GC-MS and NMR, these four polysaccharides, although they had the similarity in monosaccharide compositions of D-Man and D-Glc as well as glycosidic linkages of →4)-β-D-Man*p*-(1→ and →4)-β-D-Glc*p*-(1→, were substantive different in structural features. Firstly, the relative molecular weights of cDHPS, cDHPR, cDHPL and cDHPF were different from each other. Secondly, these four polysaccharides were composed of different monosaccharides with different molar ratios. Besides D-Man and D-Glc, cDHPR contained D-Gal and L-Ara, while cDHPL and cDHPF contained D-Gal. Thirdly, these four polysaccharides were different in glycosidic linkage types and sequences. cDHPS was a linear *O*-acetylated polysaccharide consisting of →4)-β-D-Man*p*-(1→ and →4)-β-D-Glc*p*-(1→ and acetyl groups were attached to the *O*-3 position of →4)-β-D-Man*p*-(1→. Compared to cDHPS, other polysaccharides (cDHPR, cDHPL and cDHPF) were all branched polysaccharides. For cDHPL and cDHPF, although they both were composed of a backbone consisting of →4)-β-D-Man*p*-(1→, →4)-β-D-Glc*p*-(1→ and →3,6)-β-D-Man*p*-(1→, and a branch of α-D-Gal*p*-(1→ that was attached to C-6 of →3,6)-β-D-Man*p*-(1→ in their repeat unit, the backbone of cDHPL contained acetyl groups that were attached to the *O*-3 position of →4)-β-D-Man*p*-(1→. For cDHPR, its backbone contained →4)-β-D-Man*p*-(1→, →4)-β-D-Glc*p*-(1→, →6)-α-D-Gal*p*-(1→, →4,6)-β-D-Man*p*-(1→ and →3,5)-α-L-Ara*f*-(1→, and the branches were composed of β-L-Ara*f*-(1→ that was attached to C-3 of →3,5)-α-L-Ara*f*-(1→, C-5 of →3,5)-α-L-Ara*f*-(1→and C-6 of →4,6)-β-D-Man*p*-(1→, respectively.

Previously, five polysaccharide fractions were isolated from the tissue-cultured *D. huoshanense* including protocorm-like bodies and regenerated plantlets, two from water-eluted fraction of crude polysaccharides on DEAE cellulose anion-exchange column [3,4], two from NaCl-eluted fraction of crude polysaccharides on DEAE cellulose anion-exchange column [5,6], and one from water-eluted fraction of crude polysaccharides on polyamide column [7]. As compared to the polysaccharides from stem, root, leaf and flower of cultivated *D. huoshanense*, these five polysaccharides showed obviously different structure features. Hsieh et al. reported the structure of an immunoregulatory polysaccharide from the mixed mucilage from stem and leaf of a *D. huoshanense* hybrid, which is from the hybridization of *D. huoshanense* and *D. tosaense* [22]. Although this polysaccharide was composed of →4)-β-D-Man*p*-(1→ and →4)-β-D-Glc*p*-(1→, its structure including the molar ratio of Man and Glc, relative molecular weight, the sequence of glycosyl resides and the site of acetyl groups was quite different from that of stem polysaccharide of cultivated *D. huoshanense*. These results indicated that growth pattern, environment, developmental stage and genetic background remarkably influenced the structural features of *D. huoshanense* polysaccharides.

It has been generally accepted that the biological activity of polysaccharide depends on its structural features. In the present study, based on changes in viability and apoptosis as well as *p*53 and c-myc gene expression of gastric cancer cells after polysaccharide treatment, cDHPS showed the best anti-gastric cancer activity, followed by cDHPL and cDHPF, and the anti-gastric cancer activity of cDHPR was the weakest. Undoubtedly, the different structure features of polysaccharides from stem, root, leaf and flower of *D. huoshanense* led to different anti-gastric cancer activity. Since the different parts of *D. huoshanense* have been widely used for medicinal

and edible purpose at present, our results on the different structure features and anti-gastric cancer activity of stem, root, leaf and flower polysaccharides suggested that the different parts of cultivated *D. huoshanense* should be treated differently in future applications.

5 Conclusion

The homogeneous stem, root, leaf and flower polysaccharides from cultivated *D. huoshanense* were isolated and purified, and the structural identification exhibited that there were significant differences in relative molecular weights, monosaccharide compositions, glycosidic linkage types and sequences as well as acetylated sites between these four polysaccharides. Stem polysaccharide (cDHPS) was composed of →4)-β-D-Glc*p*-(1→, →4)-β-D-Man*p*-(1→, →4)-3-*O*-acetyl-β-D-Man*p*-(1→ with the relative molecular weight of 2.59×10^5 Da, root polysaccharide (cDHPR) was composed of →3,5)-α-L-Ara*f*-(1→, →4)-β-D-Glc*p*-(1→, →4)-β-D-Man*p*-(1→, →4,6)-β-D-Man*p*-(1→, →6)-α-D-Gal*p*-(1→ and terminal β-L-Ara*f* with the relative molecular weight of 1.41×10^4 Da, leaf polysaccharide (cDHPL) was composed of →4)-β-D-Glc*p*-(1→, →4)-β-D-Man*p*-(1→, →4)-3-*O*-acetyl-β-D-Man*p*-(1→, →3,6)-β-D-Man*p*-(1→ and terminal α-D-Gal*p* with relative molecular weight of 2.09×10^5 Da, and flower polysaccharide (cDHPF) was composed of →4)-β-D-Glc*p*-(1→, →4)-β-D-Man*p*-(1→, →3,6)-β-D-Man*p*-(1→ and terminal α-D-Gal*p*-(1→ with the relative molecular weight of 4.78×10^5 Da. Among these four polysaccharides, cDHPS had the best anti-gastric cancer activity, followed by cDHPL, cDHPF and cDHPR. Further work is needed to investigate their anti-gastric cancer activity *in vivo* as well as their structure-activity relationship in order to develop functional products with suitable polysaccharides from *D. huoshanense*.

Conflicts of interest

The authors declare no competing financial interests.

Acknowledgements

This study was financially supported by the National Natural Science Foundation of China (Grant No. 31970372, 21702040) and the Fundamental Research Funds for the Central Universities (Grant No. JZ2019HGTB0065, JZ2017HGPB0169).

References

[1] J. Cheng, P. P. Dang, Z. Zhao, L. C. Yuan, Z. H. Zhou, D. Wolf, Y. B. Luo, An assessment of the Chinese medicinal *Dendrobium* industry: Supply, demand and sustainability, J. Ethnopharmacol. 229 (2019) 81–88. doi:10.1016/j.jep.2018.09.001.

[2] C. T. Lee, H. C. Kuo, Y. H. Chen, M. Y. Tsai, Current advances in the biological activity of polysaccharides in *Dendrobium* with intriguing therapeutic potential l, Curr. Med. Chem. 24 (2017) 1–1. doi:10.2174/0929867324666170227114648.

[3] X. Q. Zha, J. P. Luo, S. Z. Luo, S. T. Jiang, Structure identification of a new immunostimulating polysaccharide from the stems of *Dendrobium huoshanense*, Carbohydr. Polym. 69 (2007) 86–93. doi:10.1016/j.carbpol.2006.09.005.

[4] C. C. Tian, X. Q. Zha, L. H. Pan, J. P. Luo, Structural characterization and antioxidant activity of a low-molecular polysaccharide from *Dendrobium huoshanense*, Fitoterapia. 91 (2013) 247–255. doi:10.1016/j.fitote.2013.09.018.

[5] L. H. Pan, B. J. Feng, J. H. Wang, X. Q. Zha, J. P. Luo, Structural characterization and anti-glycation activity *in vitro* of a water-soluble polysaccharide from *Dendrobium huoshanense*, J. Food Biochem. 37 (2013) 313–321. doi:10.1111/j.1745-4514.2011.00633.x.

[6] F. Li, S. H. Cui, X. Q. Zha, V. Bansal, Y. L. Jiang, M. N. Asghar, J. H. Wang, L. H. Pan, B. F. Xu, J. P. Luo, Structure and bioactivity of a polysaccharide extracted from protocorm-like bodies of *Dendrobium huoshanense*, Int. J. Biol. Macromol. 72 (2015) 664–672. doi:10.1016/j.ijbiomac.2014.08.026.

[7] H. Y. Si, N. F. Chen, N. D. Chen, C. Huang, J. Li, H. Wang, Structural characterisation of a water-soluble polysaccharide from tissue-cultured *Dendrobium huoshanense* C.Z. Tang et S.J. Cheng, Nat. Prod. Res. 32 (2018) 252–260. doi:10.1080/14786419.2017.1350670.

[8] T F Hu. Introduction of *Dendrobium huoshanense* from wild to cultivation, J Tradit Chin Med. 4 (1958) 424,432.

[9] J. C. Ge, X. Q. Zha, C. Y. Nie, N. J. Yu, Q. M. Li, D. Y. Peng, J. Duan, L. H. Pan, J. P. Luo, Polysaccharides from *Dendrobium huoshanense* stems alleviates lung inflammation in cigarette smoke-induced mice, Carbohydr. Polym. 189 (2018) 289–295. doi:10.1016/j.carbpol.2018.02.054.

[10] M. Dubois, K. A. Gilles, J. K. Hamilton, P. A. Rebers, F. Smith., Colorimetric Method for Determination of Sugars, Anal. Chem. 28 (1956) 350–356.

[11] S. K. Gudlavalleti, A. K. Datta, Y. L. Tzeng, C. Noble, R. W. Carlson, D. S. Stephens, The Neisseria meningitidis serogroup A capsular polysaccharide O-3 and O-4 acetyltransferase, J. Biol. Chem. 279 (2004) 42765–42773. doi:10.1074/jbc.M313552200.

[12] H. Susumu, A. Eiko, S. Shigeo., O. Masahiro., K. Kazuaki., N. Jun., High-performance liquid chromatography of reducing carbohydrates as strongly ultraviolet-absorbing and electrochemically sensitive 1-phenyl-3-methyl-5-pyrazolone derivatives, Anal. Biochem. 180 (1989) 351–357. doi.org/10.1016/0003-2697(89)90444-2

[13] K. A. Kristiansen, A. Potthast, B. E. Christensen, Periodate oxidation of polysaccharides for modification of chemical and physical properties, Carbohydr. Res. 345 (2010) 1264–1271. doi:10.1016/j.carres.2010.02.011.

[14] I. Ciucanu, F. Kerek, A simple and rapid method for the permethylation of carbohydrates. Carbohydr. Res. 131 (1984) 209-217. doi.org/10.1016/0008-6215(84)85242-8.

[15] E. G. Shakhmatov, V. A. Belyy, E. N. Makarova, Structural characteristics of water-soluble polysaccharides from Norway spruce (*Picea abies*), Carbohydr. Polym. 175 (2017) 699–711. doi:10.1016/j.carbpol.2017.08.022.

[16] Y. Zhang, T. Zhou, H. Wang, Z. Cui, F. Cheng, K. P. Wang, Structural characterization and *in vitro* antitumor activity of an acidic polysaccharide from *Angelica sinensis* (Oliv.) Diels, Carbohydr. Polym. 147 (2016)

401–408. doi:10.1016/j.carbpol.2016.04.002.

[17] Y. Yuan, Y. B. Wang, Y. Jiang, K. N. Prasad, J. Yang, H. Qu, Y. Wang, Y. Jia, H. Mo, B. Yang, Structure identification of a polysaccharide purified from *Lycium barbarium* fruit, Int. J. Biol. Macromol. 82 (2016) 696–701. doi:10.1016/j.ijbiomac.2015.10.069.

[18] R. Schröder, P. Nicolas, S. J. F. Vincent, M. Fischer, S. Reymond, R. J. Redgwell, Purification and characterisation of a galactoglucomannan from kiwifruit (*Actinidia deliciosa*), Carbohydr. Res. 331 (2001) 291–306. doi:10.1016/S0008-6215(01)00046-5.

[19] I. B. Jeff, S. Li, X. Peng, R. M. R. Kassim, B. Liu, Y. Zhou, Purification, structural elucidation and antitumor activity of a novel mannogalactoglucan from the fruiting bodies of *Lentinus edodes*, Fitoterapia. 84 (2013) 338–346. doi:10.1016/j.fitote.2012.12.008.

[20] P. F. He, L. He, A. Q. Zhang, X. L. Wang, L. Qu, P. L. Sun, Structure and chain conformation of a neutral polysaccharide from sclerotia of *Polyporus umbellatus*, Carbohydr. Polym. 155 (2017) 61–67. doi:10.1016/j.carbpol.2016.08.041.

[21] Q. Li, W. Wang, Y. Zhu, Y. Chen, W. Zhang, P. Yu, G. Mao, T. Zhao, W. Feng, L. Yang, X. Wu, Structural elucidation and antioxidant activity a novel Se-polysaccharide from Se-enriched *Grifola frondosa*, Carbohydr. Polym. 161 (2017) 42–52. doi:10.1016/j.carbpol.2016.12.041.

[22] Y. S. Y. Hsieh, C. Chien, S. K. S. Liao, S. F. Liao, W. T. Hung, W. Bin Yang, C. C. Lin, T. J. R. Cheng, C. C. Chang, J. M. Fang, C. H. Wong, Structure and bioactivity of the polysaccharides in medicinal plant *Dendrobium huoshanense*, Bioorganic Med. Chem. 16 (2008) 6054–6068. doi:10.1016/j.bmc.2008.04.042

Table 1 The physicochemical properties of cDHPS, cDHPR, cDHPL and cDHPF.

Polysaccaride	Total carbohydrate (%)	O-Acetyl (%)	Average molecular weight (Da)	Monosaccharides		Glycosidic linkages	
				Sugar	Molar ratio	Type	Molar ratio
cDHPS	98.94±1.69	2.78±0.23	2.59×10^5	D-Man	3.04	1,4-linked Man*p*	2.88
				D-Glc	1.00	1,4-linked Glc*p*	1.00
cDHPR	95.09±1.36	0.65±0.09	1.41×10^4	D-Man	2.38	1,4-linked Man*p*	1.74
						1,4,6-linked Man*p*	1.00
				D-Glc	1.00	1,4-linked Glc*p*	1.52
				D-Gal	8.49	1,6-linked Gal*p*	8.37
				L-Ara	5.23	T-Ara*f*	3.55
						1,3,5-linked Ara*f*	2.41
cDHPL	96.84±1.59	1.76±0.13	2.09×10^5	D-Man	19.15	1,4-linked Man*p*	17.89
						1,3,6-linked Man*p*	1.58
				D-Glc	1.32	1,4-linked Glc*p*	1.33
				D-Gal	1.00	T-Gal*p*	1.00
cDHPF	95.47±1.74	0.39±0.11	4.78×10^5	D-Man	9.68	1,4-linked Man*p*	9.18
						1,3,6-linked Man*p*	1.12
				D-Glc	3.26	1,4-linked Glc*p*	2.65
				D-Gal	1.00	T-Gal*p*	1.00

Note: The monosaccharide of polysaccharides was detected by HPLC analysis and the results were shown in Supplemental Figure 2. The glycosidic linkages were detected by Smith degradation and methylation analysis, and the TIC profiles for Smith degradation and methylated alditol acetate analysis of polysaccharides were shown in Supplemental Figure 3 and Supplemental Figure 4, respectively.

Table 2. Chemical shift assignment of cDHPS, cDHPR, cDHPL and cDHPF.

Sugar residues		1	2	3	4	5	6
cDHPS							
(A_S) →4)-β-D-Glc*p*-(1→	C	105.49	75.49	76.77	80.24	77.72	63.12
	H	4.52	3.33	3.62	3.63	3.56	3.91/3.82
(B_S) →4)-β-D-Man*p*-(1→	C	102.87	72.61	74.82	79.18	77.77	63.07
	H	4.75	4.11	3.72	3.78	3.50	3.72/3.98
(C_S) →4)-3-*O*-acetyl-β-D-Man*p*-(1→	C	101.99	71.30	78.49	75.70	76.68	63.07
	H	4.77	4.18	4.78	3.96	3.52	3.72/3.98
cDHPR							
(A_R) →3,5)-α-L-Ara*f*-(1→	C	111.82	84.53	85.94	82.98	68.51	-
	H	5.24	3.97	3.96	4.15	3.80	-
(B_R) →4)-β-D-Glc*p*-(1→	C	105.57	75.59	76.52	80.98	77.74	63.19
	H	4.49	3.38	3.65	3.60	3.49	3.93/3.81
(C_R) →4)-β-D-Man*p*-(1→	C	102.89	72.68	74.52	79.58	77.59	63.12
	H	4.73	4.15	3.80	3.84	3.54	3.95/3.74
(D_R) β-L-Ara*f* -(1→	C	101.69	77.74	74.97	82.98	63.60	-
	H	5.02	4.09	3.96	4.11	3.74/3.77	-
(E_R) →4,6)-β-D-Man*p*-(1→	C	100.21	70.98	70.35	78.22	69.91	68.36
	H	4.57	3.96	4.08	3.77	3.78	3.95
(F_R) →6)-α-D-Gal*p*-(1→	C	98.73	70.68	69.13	68.99	71.90	66.22
	H	5.08	3.99	3.69	4.06	3.92	3.66/3.76
cDHPL							
(A_L) →4)-β-D-Glc*p*-(1→	C	105.04	75.83	76.52	79.83	77.89	63.19
	H	4.48	3.37	3.63	3.54	3.56	3.98/3.79
(B_L) →4)-β-D-Man*p*-(1→	C	102.69	72.74	74.46	79.26	77.89	63.40
	H	4.73	4.10	3.78	3.87	3.56	3.91/3.80
(C_L) →4)-3-*O*-acetyl-β-D-Man*p*-(1→	C	101.13	71.15	75.94	75.83	76.52	63.15
	H	4.82	4.19	4.83	3.95	3.50	3.93/3.77
(D_L) α-D-Gal*p*-(1→	C	96.51	67.95	69.78	69.45	71.73	61.10
	H	5.17	3.77	3.88	3.90	4.05	3.73
(E_L) →3,6)-β-D-Man*p*-(1→	C	96.35	72.05	77.53	71.04	71.84	69.56
	H	4.76	3.46	3.87	3.89	3.70	3.54
cDHPF							
(A_F) →4)-β-D-Glc*p*-(1→	C	105.11	75.97	76.19	80.72	77.66	63.13
	H	4.49	3.37	3.67	3.56	3.62	3.95/3.80
B_F) →4)-β-D-Man*p*-(1→	C	102.63	71.82	74.41	80.22	76.88	63.22
	H	4.74	4.12	3.78	3.89	3.56	3.93/3.75
(C_F) α-D-Gal*p*-(1→	C	96.30	68.26	69.94	69.66	71.32	61.23
	H	5.17	3.76	3.91	3.79	4.04	3.72
(D_F) →3,6)-β-D-Man*p*-(1→	C	96.19	71.82	77.25	71.03	71.44	69.06
	H	4.90	3.51	3.86	3.73	3.78	3.67

Fig. 1. Spectra analysis of cDHPS. A. HPGPC; B. FT-IR; C. ^{1}H NMR obtained at 298K; D. ^{1}H NMR obtained at 328K; E. ^{13}C NMR; F. HSQC; G. COSY; H. HMBC.

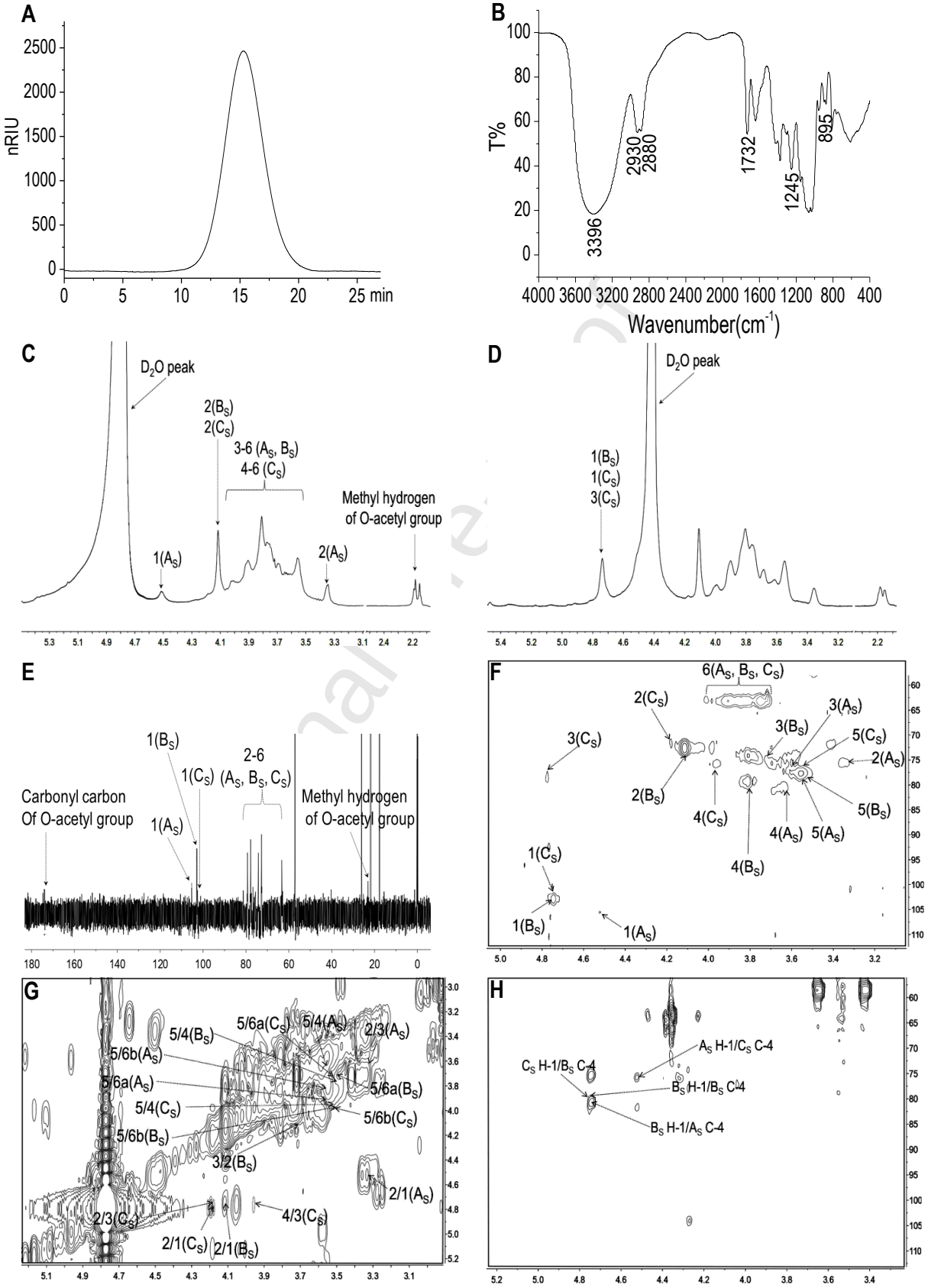

Fig. 2. Spectra analysis of cDHPR. A. HPGPC; B. FT-IR; C. ^{1}H NMR obtained at 298K; D. ^{1}H NMR obtained at 328K; E. ^{13}C NMR; F. HSQC; G. COSY; H. HMBC.

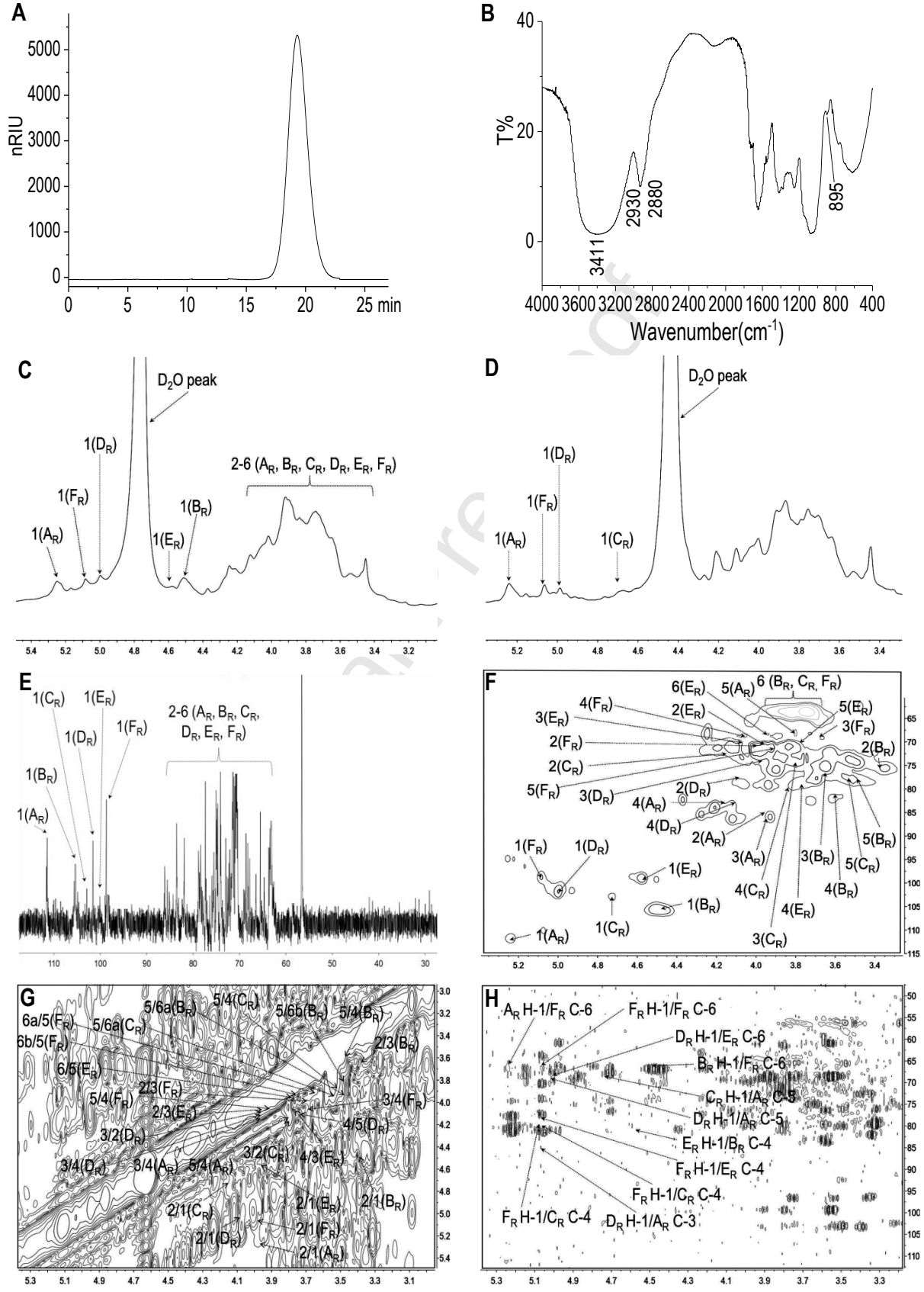

Fig. 3. Spectra analysis of cDHPL. A. HPGPC; B. FT-IR; C. ^{1}H NMR obtained at 298K; D. ^{1}H NMR obtained at 328K; E. ^{13}C NMR; F. HSQC; G. COSY; H. HMBC.

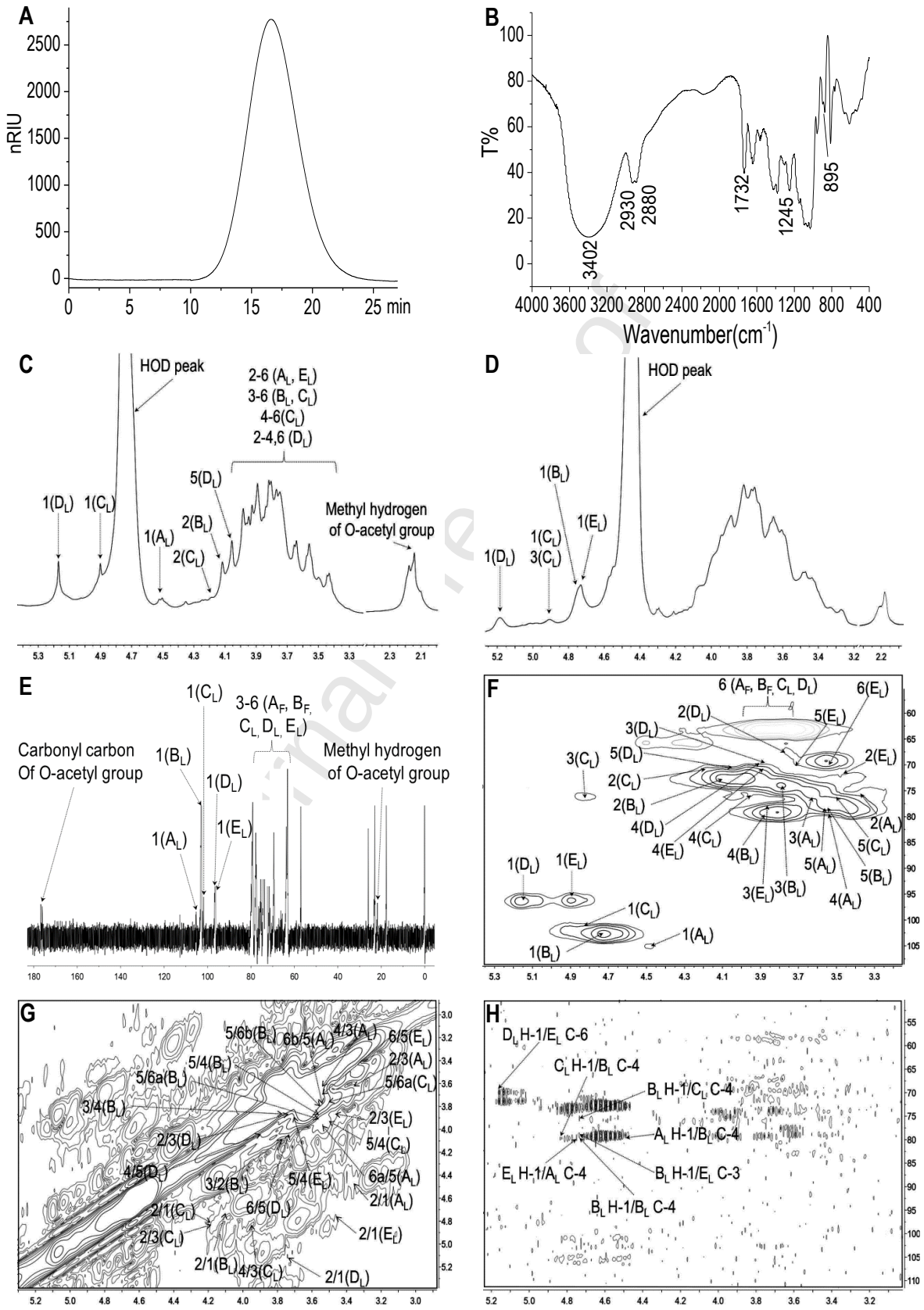

Fig. 4. Spectra analysis of cDHPR. A. HPGPC; B. FT-IR; C. ^{1}H NMR obtained at 298K; D. ^{1}H NMR obtained at 328K; E. ^{13}C NMR; F. HSQC; G. COSY; H. HMBC.

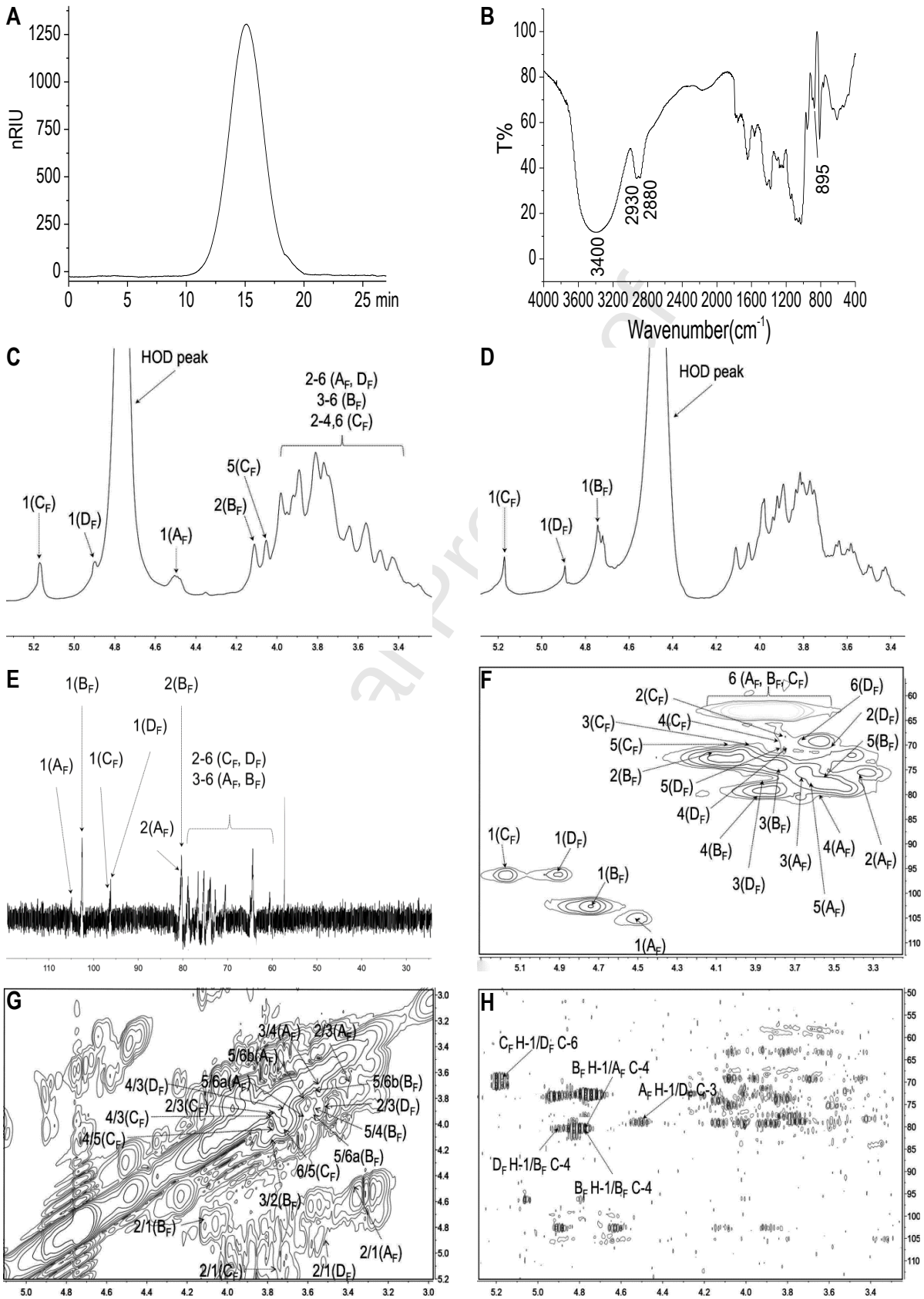

Fig. 5. Effects of different concentrations of cDHPS, cDHPR, cDHPL and cDHPF on gastric cancer cell viability. A. cDHPS; B. cDHPR; C. cDHPL; D. cDHPF. The groups without polysaccharides were used as the normal control (NC) and the group with 5-Fu was used as the positive control (PC). Different lowercase letters indicated the significant differences between groups ($p < 0.05$).

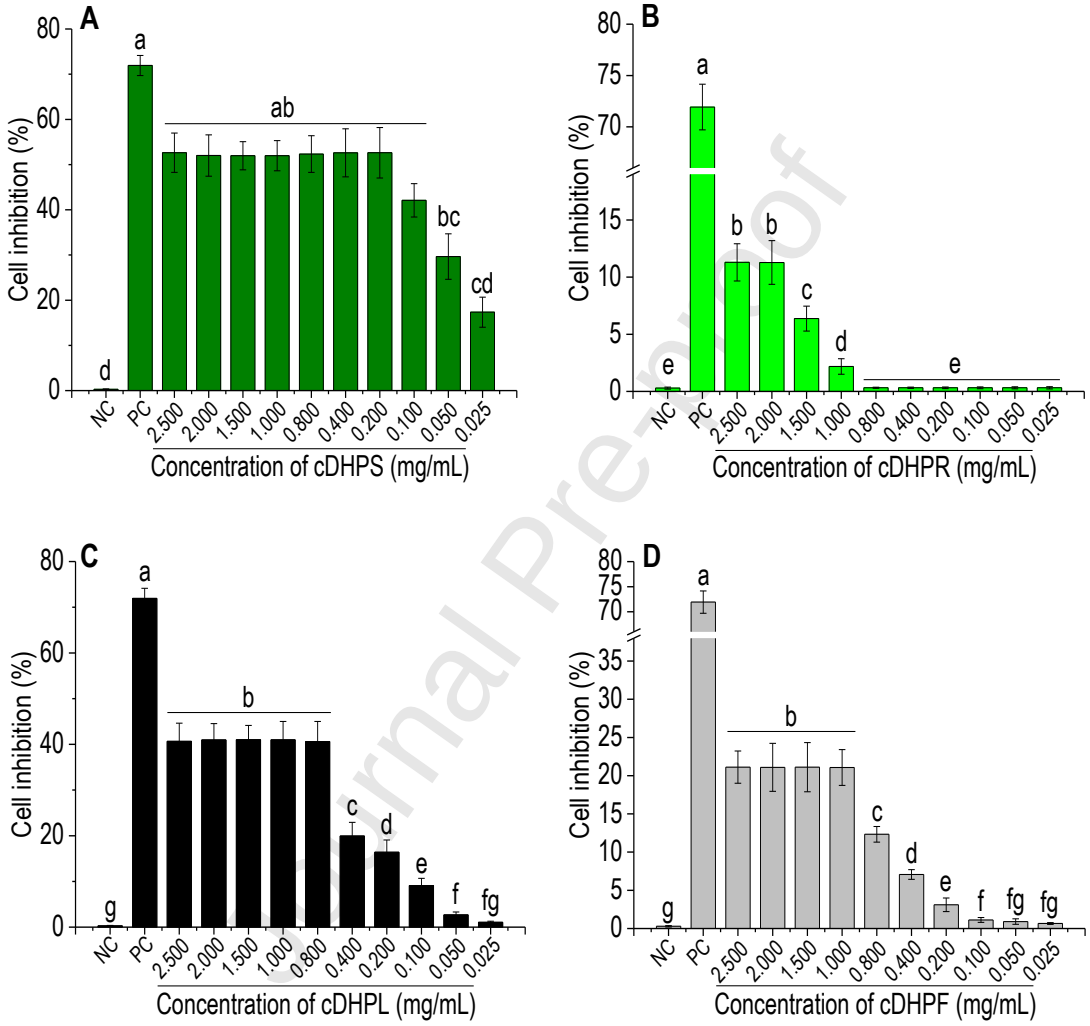

Fig. 6. Effects of different concentrations of cDHPS, cDHPR, cDHPL and cDHPF on gastric cancer cell apoptosis. A. cDHPS; B. cDHPR; C. cDHPL; D. cDHPF; E. Normal control group (NC); F. Positive control group (PC); G. The total percentages of cell apoptosis. The gastric cancer cell treated with cDHPS, cDHPR, cDHPL and cDHPF of 0.025 (a), 0.050 (b), 0.100 (c), 0.200 (d), 0.400(e), 0.800 (f), 1.000 (g), and 1.500 (h) mg/mL, respectively. $^{*}p<0.05$ or $^{**}p<0.01$ *vs*. NC. $^{\#\#}p<0.01$ *vs*. cDHPS.

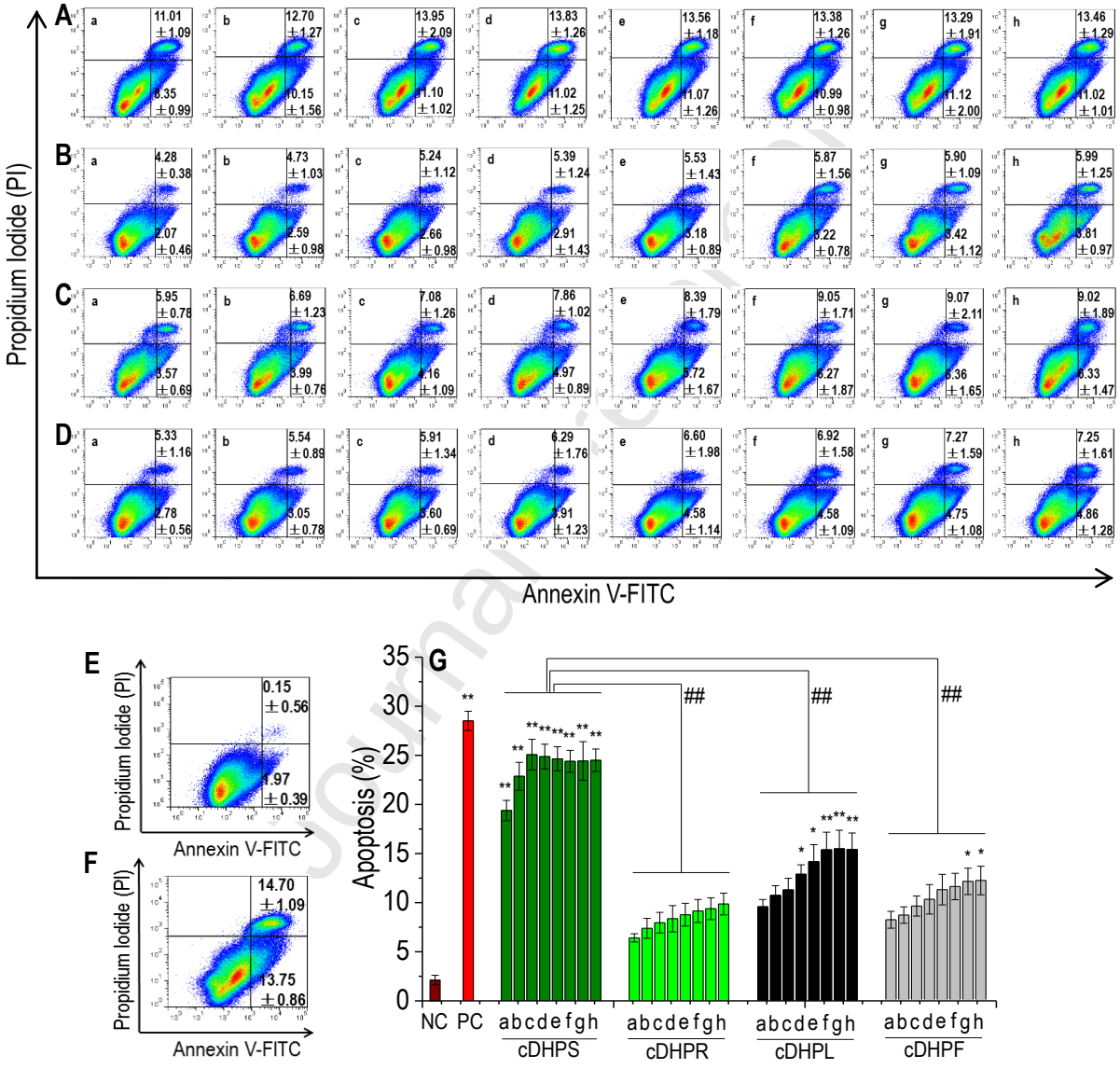

Fig. 7. Effects of different concentrations of cDHPS, cDHPR, cDHPL and cDHPF on gastric cancer cell gene expression. A. *p*53; B. c-myc. The data of mRNA level were expressed as the folds of normal control (NC). The group with 5-Fu was used as the positive control (PC). The gastric cancer cell treated with cDHPS, cDHPR, cDHPL and cDHPF of 0.025 (a), 0.050 (b), 0.100 (c), 0.200 (d), 0.400(e), 0.800 (f), 1.000 (g), and 1.500 (h) mg/mL, respectively. $^{*}p<0.05$ or $^{**}p<0.01$ *vs.* NC. $^{\#}p<0.05$ or $^{\#\#}p<0.01$ *vs*. cDHPS.

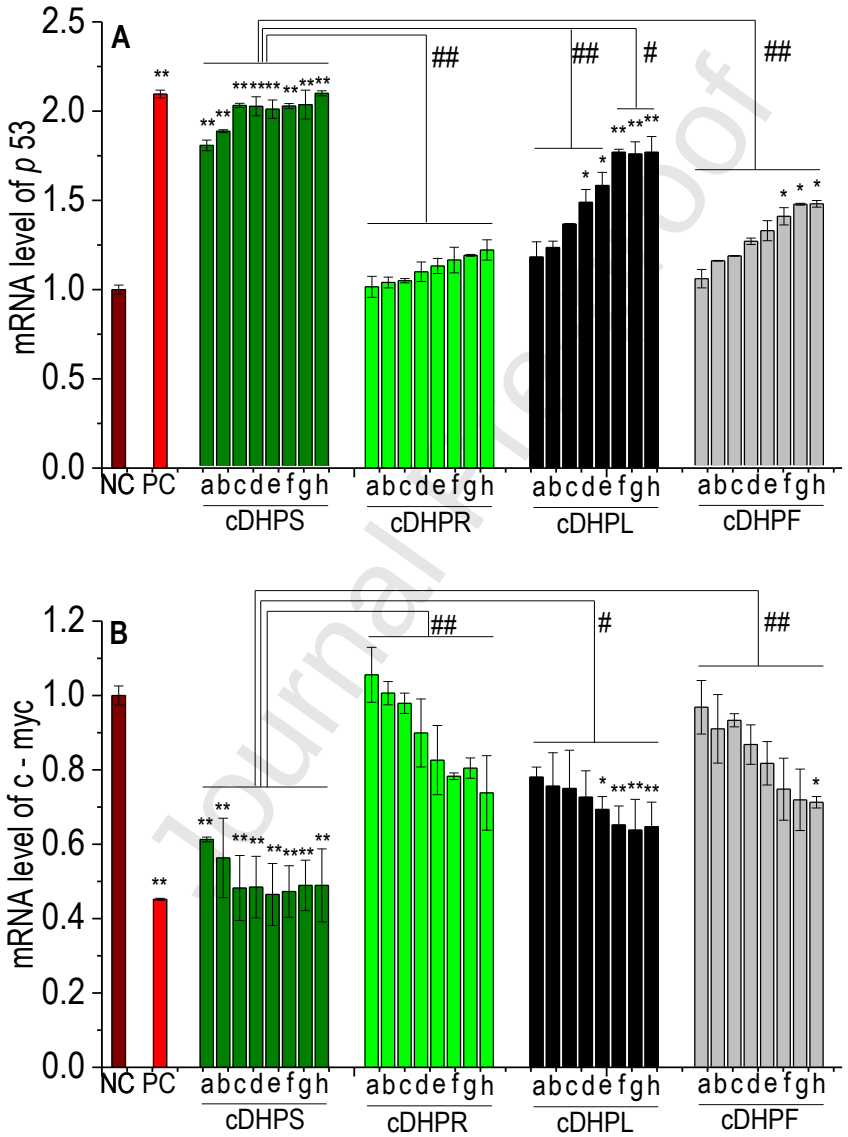

Author statement:

Bing Liu: Formal analysis, Investigation, Validation, Writing-Original Draft

Zhen-Zi Shang: Formal analysis, Investigation, Methodology

Qiang-Ming Li: Formal analysis, Project administration

Xue-Qiang Zha: Validation, Writing-Review & Editing

De-Ling Wu: Conceptualization

Nian-Jun Yu: Resources

Lan Han: Methodology, Resources

Dai-Yin Peng: Conceptualization

Jian-Ping Luo: Conceptualization, Data Curation, Supervision, Writing-Review & Editing